



Synthesis and crystal structure of a meloxicam co-crystal with benzoic acid

Christian Tantardini^{1,2} · Sergey G. Arkipov^{2,3} · Kseniya A. Cherkashina² · Alexander S. Kil'met'ev^{2,4} · Elena V. Boldyreva^{2,5}

Received: 18 June 2018 / Accepted: 16 July 2018
© Springer Science+Business Media, LLC, part of Springer Nature 2018

Abstract

Single crystals of a 1:1 co-crystal of meloxicam [4-hydroxy-2-methyl-N-(5-methyl-1,3-thiazol-2-yl)-1,1-dioxo-2H-1λ⁶,2-benzothiazine-3-carboxamide], MXM, with benzoic acid, BZA, were crystalized from a THF solution. The same MXM-BZA co-crystal has been obtained as a fine powder by liquid-assisted co-grinding using as fluid additives solvents with different polarity: benzene, toluene, ortho-xylene, meta-xylene, para-xylene, THF, and water. The latter is especially eco-friendly and can be a good candidate for industrial production. The crystal structures of all the MXM co-crystals deposited in the most recent version of the Cambridge Database were compared, in order to correlate the non-covalent interactions in these structures with the conclusions from the theoretical analysis of solubility carried out by Cysewski (J. Mol. Model 24:112, 2018).

Keywords Oxicam · Meloxicam · Solubility · Benzoic acid · Co-crystal · Co-former · Aromatic · Carboxylic acid

Introduction

Meloxicam [4-hydroxy-2-methyl-N-(5-methyl-1,3-thiazol-2-yl)-1,1-dioxo-2H-1λ⁶,2-benzothiazine-3-carboxamide], MXM, is an important active pharmaceutical ingredient (API) belonging to

oxicam family, which represents a class of nonsteroidal anti-inflammatory drugs (NSAID) that selectively inhibit COX-2 over COX-1 receptors [1, 2]. MXM co-crystallizes with different co-formers (e.g., carboxylic acids) [3–7], as other members of this family (i.e., piroxicam, tenoxicam, and lornoxicam) do [8–10]. Co-crystallization helps to improve the solubility as compared with that of pure MXM [3–6, 11, 12]. Unfortunately, not all the co-formers in these co-crystals are pharmaceutically acceptable and therefore many co-crystals cannot in fact find a real application as drug forms. One of the fortunate exceptions is a MXM co-crystal with benzoic acid (BZA). It could be used for oral administration being not human toxic. A drawback of the MXM-BZA co-crystal is that its solubility is substantially lower, than that of the other MXM co-crystals with aromatic co-formers and is very close to the solubility of MXM pure form [6]. To rationalize the aqueous dissolution behavior of MXM and its co-crystals, it is important to know the crystal structures and non-covalent interactions that hold molecules together [5, 13]. Until this work, the MXM-BZA co-crystal could be obtained only as powder and its crystal structure (and thus even its exact composition) remained unknown [3, 4].

The aim of this work was to solve for the first time the MXM-BZA crystal structure and to compare different non-covalent interactions in this co-crystal with those in pure MXM [11, 12] and its other co-crystals [4, 5, 10, 14], in order to relate the crystal structures with aqueous dissolution behavior.

Electronic supplementary material The online version of this article (<https://doi.org/10.1007/s11224-018-1166-5>) contains supplementary material, which is available to authorized users.

✉ Christian Tantardini
christiantantardini@gmail.com

✉ Sergey G. Arkipov
arksergey@gmail.com

✉ Elena V. Boldyreva
eboldyreva@yahoo.com

¹ SkolTech Skolkovo Institute of Science and Technology, ul. Nobelya 3, Moscow, Russian Federation 121205

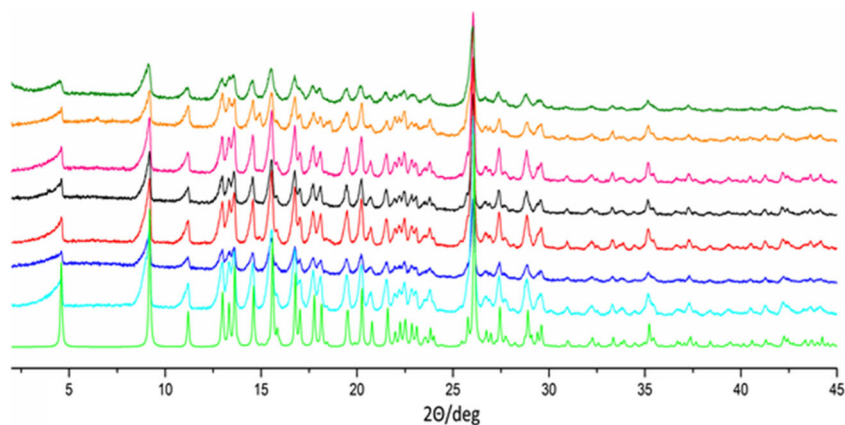
² Novosibirsk State University, ul. Pirogova 2, Novosibirsk, Russian Federation 630090

³ Institute of Solid State Chemistry and Mechanochemistry SB RAS, ul. Kutateladze 18, Novosibirsk, Russian Federation 630128

⁴ Novosibirsk Institute of Organic Chemistry SB RAS, Lavrentiev Ave. 9, Novosibirsk, Russian Federation 630090

⁵ Boreskov Institute of Catalysis SB RAS, Lavrentiev Ave. 5, Novosibirsk, Russian Federation 630090

Fig. 1 XRPD patterns of samples prepared by liquid-assisted co-grinding of MXM with BZA; fluids added: water (olive), THF (orange), orto-xylene (purple), metha-xylene (black), para-xylene (red), benzene (blue), and toluene (turquoise); for a comparison—an XRPD pattern calculated from single-crystal X-ray diffraction data (green)



Experimental

Synthesis and characterization

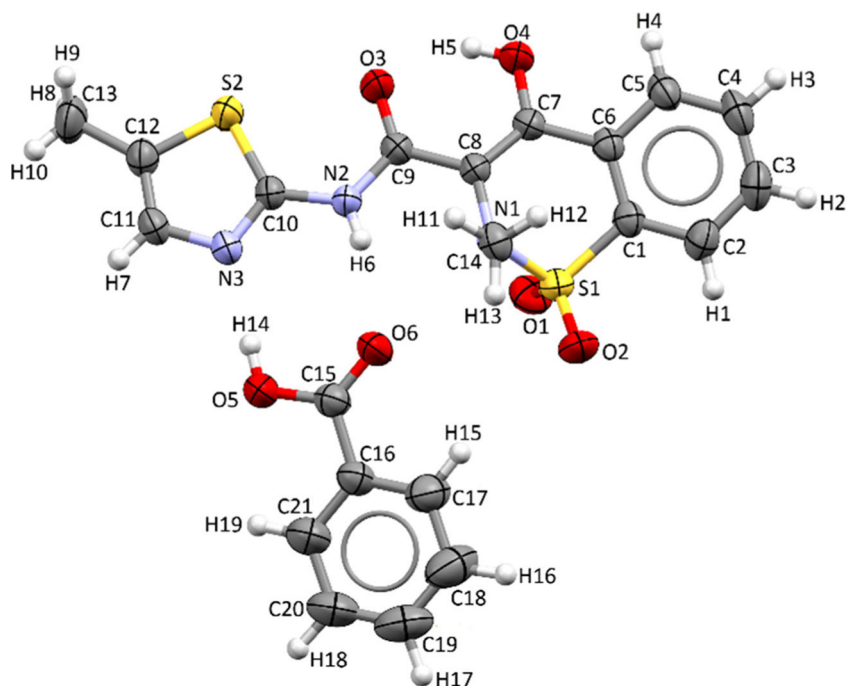
MXM and benzoic acid (purity 99%) were purchased from Sigma-Aldrich. THF, benzene, toluene, o-xylene, m-xylene, and p-xylene were purchased from Reakhim and purified

before using: THF was purified by sequential distillation over potassium hydroxide and over sodium, then distilled over sodium under an argon atmosphere; benzene and toluene were washed with concentrated sulfuric acid, then treated with potassium hydroxide, distilled over sodium, then distilled over sodium under an argon atmosphere; orto-xylene, meta-xylene, and para-xylene were distilled over sodium.

Table 1 MXM-BZA (1:1) single-crystal X-ray diffraction data collection and refinement

Crystal data	
Chemical formula	$C_{14}H_{13}N_3O_4S_2 \cdot C_7H_6O_2$
Mz	473.51
Crystal system space group	Triclinic, $P\bar{1}$
Temperature (K)	293
a, b, c (Å)	6.9679(4), 8.4287(5), 19.7001(10)
α, β, γ (°)	100.901(4), 92.770(4), 106.665(5)
V	1081.90(10)
Z	2
Radiation type	Mo $K \alpha 1$
μ (mm ⁻¹)	0.29
Crystal size (mm)	0.2 × 0.15 × 0.05
Data collection	
Diffractometer	Xcalibur, Ruby, Gemini ultra
Absorption correction	Multi-scan <i>CrysAlis PRO</i> 1.171.38.43 (Rigaku Oxford Diffraction, 2016) empirical absorption correction using spherical harmonics, implemented in SCALE3 ABSPACK scaling algorithm.
T_{min}, T_{max}	0.910, 1.000
No. of measured independent and observed [$I > 2\sigma(I)$] reflections	15,713, 3804, 2660
R_{int}	0.049
($\sin \theta/\lambda$) _{max} (Å ⁻¹)	0.595
Refinement	
$R[F^2 > 2\sigma(F^2)], wR(F^2), S$	0.042, 0.102, 1.05
No. of reflections	3804
No. of parameters	365
H-atom treatment	All H-atom parameters refined
$\Delta\rho_{max}, \Delta\rho_{min}$ (e Å ⁻³)	0.21, -0.23

Fig. 2 Asymmetric unit of the 1:1 meloxicam (MXM) co-crystal with benzoic acid (BZA), the atom-numbering scheme is shown. Displacement ellipsoids are drawn at the 50% probability level



Crystals of MXM-BZA suitable for single-crystal X-ray diffraction analysis were obtained from a THF solution by slow evaporation. The equimolar amounts (0.0001 mol of MXM and 0.0001 mol of BZA) were dissolved in 15 ml of THF. The vessel was covered by parafilm in which two small holes were made. Crystallization was carried out at room temperature. The same experiments were made with benzene, toluene, ortho-xylene, meta-xylene, and para-xylene, but no single crystals were obtained.

MXM-BZA powder samples were obtained by liquid-assisted grinding method in a Retsch CryoMill (0.0002 mol of MXM and 0.0002 BZA, room temperature, 30 min, 25 Hz).

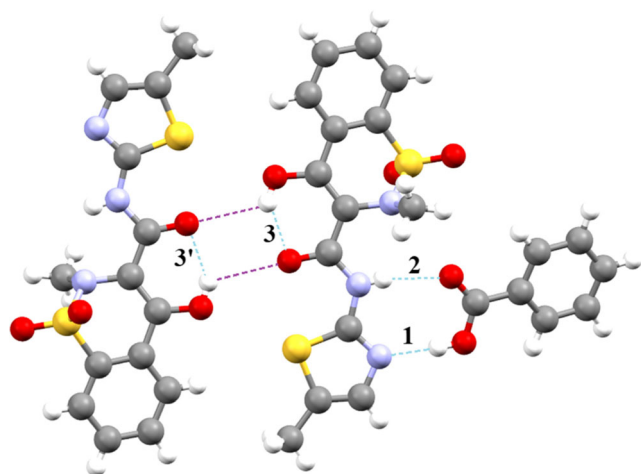


Fig. 3 A fragment of the MXM-BZA 1:1 co-crystal structure showing H-bonds in turquoise (1, 2, 3, and 3') and the long O—H...O interactions in violet

For these experiments benzene, toluene, ortho-xylene, meta-xylene, para-xylene, THF, and water were used as fluid additives in the quantity of 200 μ l for each one. The purity of samples was evaluated through X-ray determination comparing the experimental diffractograms with the theoretical pattern calculated based on single-crystal X-ray diffraction data (see Fig. 1).

X-ray diffraction structure determination

Single-crystal X-ray diffraction data for MXM:BZA (1:1) co-crystal were collected at room temperature (293 K) using an Agilent Xcalibur Ruby Gemini ultra diffractometer with Mo $K_{\alpha 1}$ radiation ($\lambda = 0.71073$ Å) and CrysAlis PRO software [15]. The crystal structure was solved using SHELXT [16] and Olex2 [17] as GUI and refined on F_{hkl}^2 with anisotropic displacement parameters for all the non-hydrogen atoms using SHELXL [16]. Hydrogen atoms positions were located from difference Fourier maps and refined freely. Olex2 [17] and

Table 2 Geometrical parameters (Å, °) for the O—H...N (1), N—H...O (2), O4—H5...O3 (3) interactions in the MXM:BZA 1:1 co-crystal (see also Fig. 3)

<i>D</i> — <i>H</i> ... <i>A</i>	<i>D</i> — <i>H</i>	<i>H</i> ... <i>A</i>	<i>D</i> ... <i>A</i>	$\widehat{D-H...A}$
O5—H14...N3 (1)	0.85(3)	1.85(3)	2.700 (3)	176 (3)
N2—H6...O6 (2)	0.77(2)	2.11(3)	2.876 (3)	168 (3)
O4—H5...O3 (3)	0.83 (3)	1.91(3)	2.619 (3)	143 (3)

Table 3 Names, stoichiometries of the asymmetric units, space symmetry groups, bi-molecular or tri-molecular clusters and common structural motifs in pure MXM and its co-crystals

Structure	Ref. code/ CSD number	Stoichiometries	Space group	Bi-/tri-/tetra	Common structural motifs
Meloxicam (MXM)	SEDZOQ/ 130826 [12] SEDZOQ01/ 107136 [11]	–	$P\bar{1}$	Bi	$R^2_2(14)$
MXM-BZA	1537194, this work	(1:1)	$P\bar{1}$	Bi	$R^2_2(8)$
Meloxicam-salicylic acid (form III)	ENICEK /819113 [4]	(1:1)	$P 2_1/c$	Bi	$R^2_2(8)$
Meloxicam-1-hydroxy-2-naphthoic acid	ENIBOT/ 819110 [4]	(1:1)	$P\bar{1}$	Bi	$R^2_2(8)$
Meloxicam-acetylsalicylic acid	ARIFOX/ 801314 [23]	(1:1)	$P 2_1/c$	Bi	$R^2_2(8)$
Meloxicam-succinic acid	ENICOU/ 819115 [4] ENICOU01/ 796926 [4]	(1:0.5)	$P\bar{1}$	Tri	$R^2_2(8) + R^2_2(8)$
Meloxicam-fumaric acid	ENICIO/ 819114 [6]	(1:0.5)	$P\bar{1}$	Tri	$R^2_2(8) + R^2_2(8)$
Meloxicam-acetylendicarboxylic acid	EBOLEP/ 1506179 [24]	(1:0.5)	$P\bar{1}$	Tri	$R^2_2(8) + R^2_2(8)$
Meloxicam-glutaric acid	ENIBUZ/ 819111 [4]	(1:1)	$P\bar{1}$	Tetra	$R^2_2(8) + R^2_2(8) + R^2_2(8)$
Meloxicam-adipic acid	FAKJOS/ 834808 [5]	(1:0.5)	$P\bar{1}$	Tri	$R^2_2(8) + R^2_2(8)$
Meloxicam-terephthalic acid	FAKJUY/ 834809 [5]	(1:0.5)	$P\bar{1}$	Tri	$R^2_2(8) + R^2_2(8)$

Table 4 Comparison of the geometrical parameters of the H-bonds and O...O interactions in meloxicam and its co-crystals

Structure	Ref. code/ CSD number	N—H...O, Å	N—H...O, °	O—H...N, Å	O—H...N, °	O...O, Å	O...O, °
Meloxicam (MXM)	SEDZOQ/ 130826 [12]	3.035(3)	167(3)	–	–	3.236(2)	129(4)
	SEDZOQ01/ 107136 [11]	O from S-O group 3.028(2)	166(3)	–	–	3.232(2)	115(3)
MXM-BZA	1537194, this work	O from S-O group 2.876(3)	168(3)	2.700(3)	176(3)	3.086(2)	121(3)
Meloxicam-salicylic acid (form III)	ENICEK /819113 [4]	2.968(3)	163.8	2.968(3)	170.4	–	–
Meloxicam-1-hydroxy-2-naphthoic acid	ENIBOT/ 819110 [4]	2.901(3)	166.5	2.563(3)	172.2	3.055(2)	117.9
Meloxicam-acetylsalicylic acid	ARIFOX/ 801314 [23]	2.858(3)	165.5	2.666(3)	174.2	–	–
Meloxicam-succinic acid	ENICOU/ 819115 [4]	2.871(2)	167(2)	2.697(2)	166(2)	2.935(1)	112(2)
	ENICOU01/ 796926 [4]	2.850(4)	164.3	2.683(4)	173.6	2.893(4)	115.2
Meloxicam-fumaric acid	ENICIO/ 819114 [6]	2.857(4)	160(3)	2.658(3)	174.4	2.902(3)	114.7
Meloxicam-acetylendicarboxylic acid	EBOLEP/ 1506179 [24]	2.922(3)	163.7	2.615(3)	174.5	2.943(2)	114.4
Meloxicam-glutaric acid	ENIBUZ/ 819111 [4]	2.839(2)	164.9	2.668(2)	173.96	2.907(2)	115.64
Meloxicam-adipic acid	FAKJOS/ 834808 [5]	2.866(3)	163(2)	2.663(3)	173(4)	–	–
Meloxicam-terephthalic acid-	FAKJUY/ 834809 [5]	2.984(2)	162(2)	2.639(2)	175(3)	–	–

Table 5 Centroid-topocentroid distances (up to 5 Å) and dihedral angles in the meloxicam co-crystals and pure meloxicam

Structure	Ref. code/ CSD number	Type of centroids	Distance between ring centroids, Å	Dihedral angle between planes formed by centroids, °
MXM-BZA	1537194, this work	THY...THY	3.7308(15)	12.06(13)
		AR-BZA AR-BZA	4.207(2)	0.00(18)
		THY...BZR	4.3977(15)	12.06(13)
Meloxicam-salicylic acid (form III)	ENICEK /819113 [4]	THY...AR	3.9539(18)	11.31(16)
		AR...AR	4.424(2)	0.02(17)
Meloxicam-1-hydroxy-2-naphthoic acid	ENIBOT/ 819110 [4]	THY...AR1	3.739(2)	3.07(13)
		BZR...AR2	3.893(2)	17.48(13)
		BZR...AR	4.236(3)	17.48(13)
		THY...AR	4.975(3)	4.93(14)
Meloxicam-acetylsalicylic acid	ARIFOX/ 801314 [23]	THY...AR	3.7399(15)	6.37(12)
		THY...BZR	4.4354(15)	24.04(13)
		THY...THY	4.1287(7)	0.02(7)
Meloxicam-succinic acid	ENICOU01/ 796926 [4]	THY...BZR	3.7992(8)	5.53(7)
		THY...THY	4.1287(7)	0.02(7)
		THY...BZR	3.730(2)	4.66(19)
Meloxicam-fumaric acid	ENICIO/ 819114 [6]	THY...BZR	3.785(3)	3.81(14)
		THY...THY	4.104(3)	0.03(14)
		THY...BZR	3.7383(12)	6.68(11)
Meloxicam-acetylenedicarboxylic acid	EBOLEP/ 1506179 [24]	THY...BZR	3.7383(12)	6.68(11)
		THY...THY	4.1139(11)	0.00(10)
Meloxicam-glutaric acid	ENIBUZ/ 819111 [4]	THY...BZR	3.7542(16)	4.47(8)
		THY...THY	4.0222(17)	0.00(8)
Meloxicam-adipic acid	FAKJOS/ 834808 [5]	THY...BZR	4.6829(14)	24.04(11)
		THY...BZR	4.7330(16)	24.04(11)
Meloxicam-terephthalic acid	FAKJUY/ 834809 [5]	THY...BZR	4.5640(11)	20.18(9)
		THY...BZR	4.6658(11)	20.18(9)
Meloxicam	SEDZOQ/ 130826 [12]	THY...BZR	3.7440(16)	11.84(13)
		THY...BZR	4.2123(16)	11.84(13)
	SEDZOQ01/ 107136 [11]	THY...BZR	3.7498(17)	11.70(14)
		THY...BZR	4.2161(18)	11.70(14)

Mercury [18] were used to visualize the structures and to prepare the material for publication. The parameters characterizing data collection and refinement are summarized in Table 1.

All powder samples were characterized by XRPD using a Stoe Stadi-MP diffractometer with Cu K α 1 radiation ($\lambda = 1.54060$ Å) at operating potential of 40 kV and electric current of 40 mA, and a Mythen 1 K detector. All data were processed using WinXPOW [19] and Origin programs. XRPD patterns of the co-crystal sample were compared with the patterns of the starting reactants, MXM (CSD Refcode: SEDZOQ [12]), BZA (CSD Refcode: BENZAC02 [20]), and powder pattern calculated from MXM-BZA single-crystal X-ray diffraction data (CSD Refcode: 1537194, this work) to prove the formation of the MXM-BZA co-crystal (Fig. 1).

Results and discussion

The asymmetric unit of the MXM-BZA co-crystal is shown in Fig. 2. The structure crystallizes in a triclinic $P\bar{1}$ space symmetry group.

A fragment of molecular structure is shown in Fig. 3, describing the typical NCI which are classified as H-bonds based on the geometrical criteria provided by Arunan et al. [21]. The components of the MXM-BZA structure are linked into a bimolecular cluster via the O—H...N (**1**) and N—H...O (**2**) hydrogen bonds (H-bonds) between MXM and BZA (see Table 2), to form a R_2^2 (8) ring (notations are as in Bernstein et al. [22]). Furthermore, there are long O—H...O interactions formed by the carbonyl and hydroxyl groups of the two MXM molecules, these groups

being already involved into the O—H...O (3, 3') intramolecular H-bond (see Table 2).

Molecular packing and NCI in the MXM-BZA co-crystal can be compared with those in pure MXM and in the other MXM co-crystals (Tables 3, 4, and 5).

The MXM co-crystals can be classified into two groups depending on whether the co-former is a monocarboxylic or a dicarboxylic acid. In both groups, one can find aromatic carboxylic acids among co-formers: salicylic acid; 1-hydroxy-2-naphthoic acid; acetylsalicylic acid; terephthalic acid; benzoic acid (the structure solved in this work for the first time). Four of these co-formers are monocarboxylic acids, while the terephthalic acid is a dicarboxylic one.

The asymmetric units of co-crystals with monocarboxylic acids contain two molecules: MXM and a co-former (Fig. 2). Within this group, co-crystals of MXM with BZA and with 1-hydroxy-2-naphthoic acid have triclinic $P\bar{1}$ space symmetry, while co-crystals of MXM with salicylic acid (form III), and with acetylsalicylic acid, are monoclinic ($P2_1/c$ space symmetry). Structural motifs in MXM-BZA co-crystal are similar to those in the MXM co-crystal with 1-hydroxy-2-naphthoic acid; while MXM co-crystals with acetylsalicylic acid and salicylic acid form bimolecular clusters via O—H...N and N—H...O H-bonds between MXM and co-former, to give R_2^2 (8) rings.

Co-crystals of MXM with dicarboxylic acids contain one MXM molecule and a half of the co-former molecule in the asymmetric unit (Fig. 4). Within such co-crystals the components are linked into tri-molecular clusters via the O—H...N and N—H...O H-bonds between two carboxylic groups belonging to a co-former and two MXM molecules, to form two R_2^2 (8) rings [6].

The only known exception from this general trend is a co-crystal of MXM with glutaric acid (GLU), in which the asymmetric unit has two molecules: a MXM and a co-former. The components are linked into tetra-molecular clusters MXM:GLU:GLU:MXM with O—H...N and N—H...O H-bonds between MXM and GLU, to form R_2^2 (8) rings, and O—H...O H-bonds between two GLU molecules, also to form R_2^2 (8) rings (Fig. 5).

The analysis of different NCIs within pure MXM and its co-crystals shows that monocarboxylic acids form similar O—H...N and N—H...O H-bonds with a MXM molecule. What differentiates pure MXM structure and its co-crystals with monocarboxylic acids are the $\pi... \pi$ interactions. A MXM molecule itself has two aromatic fragments: thiazole (THY) and benzene (BZR) rings. These aromatic fragments can participate in the $\pi... \pi$ interactions both in pure MXM and in its co-crystals. The THY...BZR $\pi... \pi$ interactions are present in pure MXM and its co-crystals with non-aromatic acids, as well as with such aromatic acids as benzoic, acetylsalicylic, and terephthalic acids (Fig. 6e, b, c). The THY...THY $\pi... \pi$

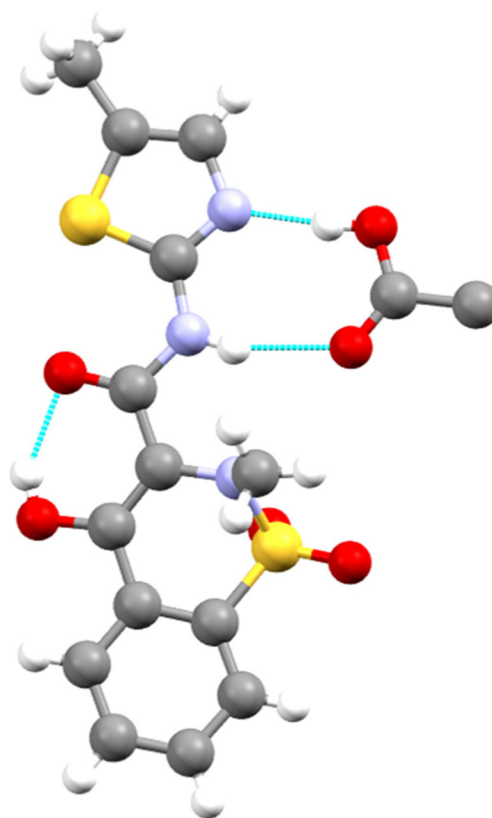


Fig. 4 Asymmetric unit of the 1:0.5 meloxicam (MXM) co-crystal with acetylenedicarboxylic acid (ACA), H-bonds are shown turquoise

interactions are present in the MXM co-crystals with non-aromatic acids, the co-crystal with the adipic acid being the only known exception.

THY and BZR are responsible also for the $\pi... \pi$ interactions with the aromatic ring (AR) belonging to co-former aromatic acids: THY...AR $\pi... \pi$ interaction are present in the MXM co-crystals with salicylic, 1-hydroxy-2-naphthoic, acetylsalicylic, and benzoic acids (Fig. 6a, b, e); BZR...AR $\pi... \pi$ interactions are present in the MXM co-crystals with 1-hydroxy-2-naphthoic acid (Fig. 6a).

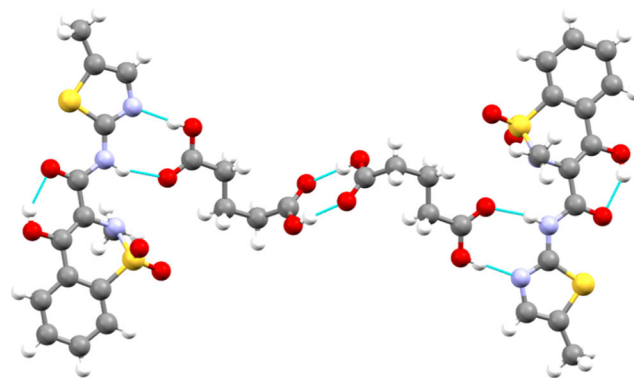


Fig. 5 A tetra-molecular cluster within the meloxicam (MXM) co-crystal with glutaric acid (GLU), H-bonds are shown in turquoise

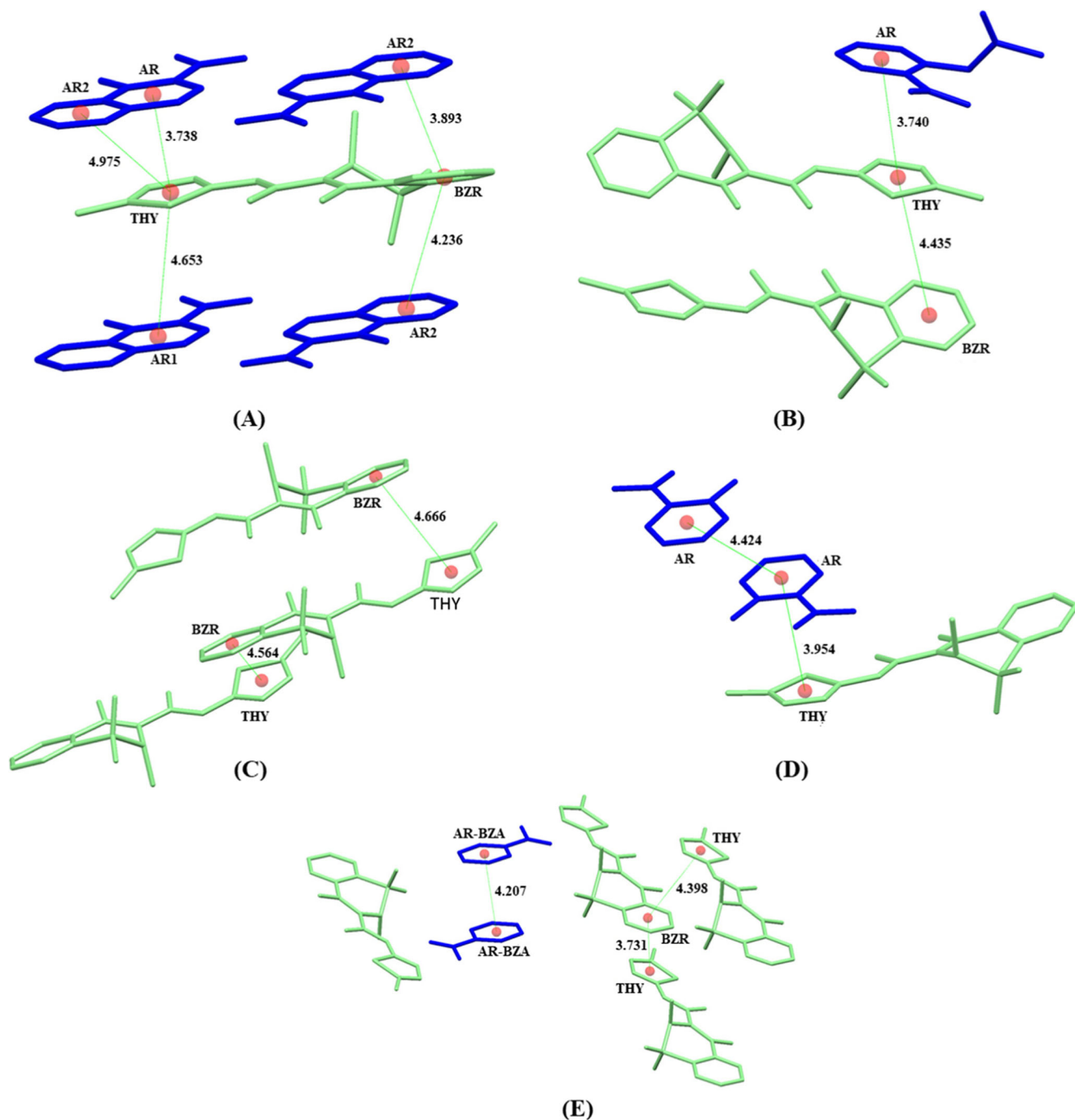


Fig. 6 Centroid/topocentroid (red balls) distances (Å) within MXM co-crystals with **a** 1-hydroxy-2-naphthoic acid [4], **b** acetylsalicylic acid [23], **c** terephthalic acid [5], **d** salicylic acid (form III) [4], and **e** BZA (this work)

These $\pi\cdots\pi$ interactions are not considered for the MXM co-crystal with terephthalic acid, because the distances between centroids (topocentroids¹) between $\text{THY}\cdots\text{AR}$ and $\text{BZR}\cdots\text{AR}$ in this structure exceed 5 Å, that was considered as the upper limit for a possible $\pi\cdots\pi$ interaction.

¹ A topocentroid is a topological index that is calculated for a group of 5-atoms as proposed by Cremer et al. [25] and 6-atoms as proposed by Boeyens et al. [26].

$\text{AR}\cdots\text{AR}$ $\pi\cdots\pi$ interactions are present also in the MXM co-crystals with salicylic and benzoic acids.

Conclusions

Recently, intermolecular interactions were considered as a direct measure of water solubility advantage of meloxicam cocrystallized with carboxylic acids [1]. It was argued that

solubility can be quantified by concentration of pairs of molecules formed in water. Extending this approach, one can compare the molecular clusters present in the crystalline state, prior to breaking the NCI as a result of the interaction with the solvent molecules. One can then notice that in the case of MXM co-crystals with non-aromatic carboxylic acids, both H-bonds and $\pi\cdots\pi$ interactions are similar and the different solubility behavior can be related to the different carbon chain length of the carboxylic acids. In the case of the MXM co-crystals with aromatic carboxylic acids, the H-bonds are similar, but $\pi\cdots\pi$ interactions are different, and this latter difference can account for the differences in the dissolution behavior. Both observations agree with the model proposed by Cysewski 2018 [13].

Earlier [5], the increase in the solubility of MXM co-crystals with dicarboxylic acids was supposed to be a consequence of the change in the intermolecular interactions in the solid when the dimers of MXM molecules (present in pure MXM) are broken by dicarboxylic acid molecules and the contact with solvent molecules is facilitated. A theoretical study by Cysewski [13] attempted to correlate aqueous dissolution of MXM co-crystals with the presence of certain molecular clusters in solution. The comparison of the solubilities of the crystalline co-crystals with aromatic and non-aromatic co-formers suggests that aqueous dissolution behavior of MXM co-crystals correlates also with the presence or the absence of the $\pi\cdots\pi$ interactions in the crystal structure. The solubility is higher for those structures, in which there are the $\pi\cdots\pi$ interactions between AR and MXM, like in most co-crystals with aromatic co-formers [4]. In the MXM-BZA co-crystal, these interactions are absent, and the solubility of this co-crystal is almost as low, as that of the pure MXM. This suggests, that for a higher aqueous solubility, it is important not only that the interactions between the MXM molecules in the crystals are weakened, as supposed in [5], but also that a complex formed by a MXM molecule and a co-former is preserved in solution, as modeled in [13]. In the case of MXM-BZA co-crystals, the weakness of the $\pi\cdots\pi$ interactions between the MXM and the BZA molecules prevents the formation of such a complex in solution, and the solubility falls down, almost to the level of pure MXM.

Acknowledgments The authors received funding from the Russian Ministry of Science and Higher Education.

Compliance with ethical standards

Conflict of interest The authors declare that they have no conflict of interest.

References

1. Furst DE (1997). *Semin Arthritis Rheum* 26:21
2. Schattenkirchner M (1997) *Expert. Opin. Investig. Drugs* 6:321
3. Myz SA, Shakhtshneider TP, Fucke K, Fedotov AP, Boldyreva EV, Boldyrev VV, Kuleshova NI (2009). *Mendeleev Communications* 19:272
4. Cheney ML, Weyna DR, Shan N, Hanna M, Wojtas L, Zaworotko MJ (2010). *Cryst Growth Des* 10:4401
5. Tumanov NA, Myz SA, Shakhtshneider TP, Boldyreva EV (2012). *CrystEngComm* 14:305–313
6. Weyna DR, Cheney ML, Shan N, Hanna M, Zaworotko MJ, Sava V, Song S, Sanchez-Ramos JR (2012). *Mol Pharm* 9:2094
7. Myz SA, Shakhtshneider TP, Tumanov NA, Boldyreva EV (2012). *Russ Chem Bull* 9:1782
8. Fucke K, Myz SA, Shakhtshneider TP, Boldyreva EV, Griesser UJ (2012). *New J Chem* 36:1969
9. Bolla G, Sanphui P, Nangia A (2013). *Cryst Growth Des* 13:1988
10. Suresh K, Nangia A (2014). *Cryst Growth Des* 14:2945
11. Luger P, Daneck K, Engel W, Trummelitz G, Wagner K (1996). *Eur J Pharm Sci* 4:175
12. Fabiola GF, Pattabhi V, Manjunatha SG, Rao GV, Nagarajan K (1998) *Acta Crystallogr. Sect C* 54:2001
13. Cysewski P (2018). *J Mol Model* 24:112
14. Uhlemann T, Seidel S, Müller CW (2017). *Phys Chem Chem Phys* 19:14625
15. Rigaku OD (2016). *CrysAlis PRO*. Rigaku Oxford diffraction Ltd, Yarnton
16. Sheldrick GM (2015). *Acta Cryst. C* 71:3
17. Dolomanov OV, Bourhis LJ, Gildea RJ, Howard JAK, Puschmann H (2009). *J Appl Crystallogr* 42:339
18. Macrae CF, Bruno IJ, Chisholm JA, Edgington PR, McCabe P, Pidcock E, Rodriguez-Monge L, Taylor R, van de Streek J, Wood PA (2008). *J Appl Crystallogr* 41:466
19. Stoe & Cie (1999) *WinXPow*. Stoe & Cie, Darmstadt
20. Feld R, Lehmann MS, Muir KW, Speakman JC (1981). *K Zeitschrift für Kristallographie* 157:215
21. Arunan E, Desiraju GR, Klein RA, Sadlej J, Scheiner S, Alkorta I, Clary DC, Crabtree RH, Dannenberg JJ, Hobza P, Kjaergaard HG, Legon AC, Mennucci B, Nesbitt DJ (2011) *Pure Appl. Chem* 83:1637
22. Bernstein J, Davis RE, Shimoni L, Chang NL (1995). *Angew Chem Int Ed Engl* 34:1555
23. Cheney ML, Weyna DR, Shan N, Hanna M, Wojtas L, Zaworotko MJ (2011). *J Pharm Sci* 100:2172
24. Tantardini C, Arkhipov SG, Cherkashina KA, Kil'met'ev AS, Boldyreva EV (2016). *Acta Cryst. E* 72:1856
25. Cremer D, Pople JA (1975). *J Amer Chem Soc* 97:1354
26. Boeyens JCA (1978). *J Cryst Mol Struct* 8:317